

Structural Time-dependent Reliability Assessment with A New Power Spectral Density Function

Cao Wang, S.M.ASCE¹, Hao Zhang, M.ASCE² and Michael Beer, Dr.Eng., M.ASCE³

ABSTRACT

An important ingredient of time-dependent reliability analysis of civil structures is to choose a proper model for the applied loads. The stochastic process theory has been widely used in existing studies to perform structural time-dependent reliability analysis. However, the use of many types of power spectral density function leads to an inefficient calculation of structural reliability. This paper proposes an analytical method for structural reliability assessment, where a new power spectral density function is developed to enable the reliability analysis to be conducted with a simple and efficient formula. A non-Gaussian load process, if present, is first converted into an “equivalent” Gaussian process to improve the assessment accuracy. Illustrative examples are presented to demonstrate the applicability of the proposed method. Results show that a greater autocorrelation in the load process leads to a smaller failure probability. The structural reliability may be significantly overestimated if one simply treats the non-Gaussian load process as a Gaussian one. Moreover, the impact of modeling the load process as a continuous process or a discrete one on structural reliability is also investigated.

¹Ph.D. student, School of Civil Engineering, Univ. of Sydney, Sydney, NSW 2006, Australia. ORCID: <http://orcid.org/0000-0002-2802-1394>. Email: cao.wang@sydney.edu.au

²Associate Professor, School of Civil Engineering, Univ. of Sydney, Sydney, NSW 2006, Australia (corresponding author). Email: hao.zhang@sydney.edu.au

³Professor of Uncertainty in Engineering and Head, Institute for Risk and Reliability, Leibniz Univ. Hannover, 30167 Hannover, Germany; Institute for Risk and Uncertainty, Univ. of Liverpool, Liverpool L69 3BX, United Kingdom; International Joint Research Center for Engineering Reliability and Stochastic Mechanics (ERSM), Tongji Univ., Shanghai 200092, China. E-mail: beer@irz.uni-hannover.de

1 **Keywords:** Time dependent reliability; Stochastic process; Outcrossing rate; Load autocor-
2 relation

3 INTRODUCTION

4 Civil structures and infrastructures are subjected to both environmental attacks (e.g.,
5 Chloride-induced corrosion to RC structures) and severe load effects (e.g., over-weighted
6 traffic loads to bridges) during their service life. Such factors may essentially impair the
7 structural service reliability. A probability-based approach should be used to evaluate the
8 serviceability level and remaining life of an engineered structure (Mori and Ellingwood 1993;
9 Enright and Frangopol 1998; Akiyama and Frangopol 2014; Wang et al. 2017). The basic
10 concept of structural reliability assessment is to examine whether the load effect (\mathcal{S}) exceeds
11 the structural resistance (load-bearing capacity, \mathcal{R}). Both \mathcal{R} and \mathcal{S} are practically uncertain
12 due to the randomness arising from structural geometry, material strength, load volume, and
13 others. Mathematically, the structural failure probability, \mathbb{P} , is estimated by $\mathbb{P} = \Pr(\mathcal{R} - \mathcal{S} <$
14 $0)$, where \Pr denotes the probability of the event in the bracket. For the reliability assessment
15 of a structure within a specific reference period (e.g., during its lifetime), however, both the
16 resistance and the external loads may vary with time and thus cannot be simply represented
17 by a single random variable. Under this context, let $\mathcal{R}(t)$ and $\mathcal{S}(t)$ denote the resistance and
18 load effect at time t , respectively. The time-dependent reliability within a service period of
19 $[0, T]$, $\mathbb{L}(T)$, is given by

$$\mathbb{L}(T) = \Pr \{ \mathcal{R}(t) > \mathcal{S}(t), \forall t \in [0, T] \} = \int_0^T \int_{Z(t) > 0} f_{Z(t)}(z(t)) d[z(t)] dt \quad (1)$$

20 where $Z(t) = \mathcal{R}(t) - \mathcal{S}(t)$ is the limit state function at time t , and $f_{Z(t)}$ is the probability
21 density function (PDF) of $Z(t)$, which also varies with t . By definition, the time-dependent
22 failure probability, $\mathbb{P}(T)$, is the complementary of $\mathbb{L}(T)$, i.e., $\mathbb{P}(T) = 1 - \mathbb{L}(T)$. Note that
23 Eq. (1) indeed involves a multi-fold integral, as well as the potential association between
24 different folds, and thus is often difficult or even impossible to solve directly. Specifically,

25 in terms of the external loads, both the non-stationarity and the temporal autocorrelation
 26 should be considered in a reasonable manner. As such, some simplifications have been
 27 introduced to achieve a practical yet sufficiently accurate solution to the reliability problem
 28 (Mori and Ellingwood 1993; Melchers 1999; Li et al. 2005; Li et al. 2015; Wang et al. 2016;
 29 Wang and Zhang 2018). One of the existing methods to model the external loads is to
 30 employ a discrete stochastic process (e.g., a Poisson process) to represent the occurrence of
 31 significant loads that may impair structural safety directly. A remarkable work was done by
 32 Mori and Ellingwood (1993), who considered a stationary Poisson process for the loads, and
 33 proposed a closed-form solution for structural time-dependent reliability,

$$\mathbb{L}(T) = \exp \left\{ \lambda \int_0^T F_S[r_0 \cdot g(t)] dt - \lambda T \right\} \quad (2)$$

34 where r_0 is the initial resistance, λ is the mean occurrence rate of the Poisson process (i.e.,
 35 on average λ event(s) occurs within a unit time), F_S is the cumulative density function
 36 (CDF) of each load effect, and $g(t)$ is the deterioration function of resistance (i.e., the
 37 ratio of resistance at time t to the initial resistance). Li et al. (2015) further proposed a
 38 generalized form of Eq. (2), where the non-stationarity in the load stochastic process was
 39 also considered. Moreover, note that the autocorrelation in the load process also arises
 40 due to common physical-based causes (e.g., Ellingwood and Lee 2016). Conceptually, the
 41 correlation between two load effects at two different time points is expected to decrease as
 42 the time separation increases. A frequently-used model takes the form of (e.g., Li et al.
 43 2016b)

$$\rho(\tau) = \exp(-k \cdot \Delta\tau) = \exp(-k|\tau_1 - \tau_2|) \quad (3)$$

44 where $\rho(\tau)$ is the linear correlation coefficient between two loads with a time separation (or a
 45 spatial distance) of $\Delta\tau$, k is the scale factor accounting for the correlation changing rate, τ_1
 46 and τ_2 are the two occurring times of loads. Eq. (3) is, however, only valid for a continuous
 47 process as a discrete load process is unavoidably associated with intermittence. Wang and

48 [Zhang \(2018\)](#) proposed a model to describe the autocorrelation in a discrete process, and
49 investigated the impact of load temporal correlation on structural time-dependent reliability.
50 [Ellingwood and Lee \(2016\)](#) studied the autocorrelation in the hurricane wind process, where
51 an auto-regressive model was used to measure the autocorrelation in the wind loads.

52 The aforementioned discrete load processes, however, may fail to describe the cases where
53 the load effect is applied continuously to a structure (e.g., underground poles subjected to
54 earth pressure). Fig. 1 shows a conceptual comparison between a continuous load process
55 (Fig. 1(a)) and a discrete one (Fig. 1(b)). For use in structural reliability assessment, a
56 continuous load process could be transformed to a discrete one, where only the significant
57 load events (e.g., with a magnitude that exceeds a pre-defined threshold) are considered.
58 While this approach has been used in the literature (e.g., [Mori and Ellingwood 1993](#); [Li
59 et al. 2015](#)), the error induced by such an approximation in structural reliability remains
60 unaddressed.

61 For a continuous load process which is applied uninterruptedly, the main characteristics
62 of the process can be captured by the statistics including the mean value, variance and au-
63 tocorrelation. Further, the structural time-dependent reliability analysis can be transformed
64 into a problem of a stochastic process crossing a predefined barrier level (e.g., the resistance)
65 ([Grigoriu 1984](#); [Engelund et al. 1995](#); [Li et al. 2016b](#)). The solution is usually referred to
66 as “first passage probability”. This method has been widely used in the literature to esti-
67 mate the reliability of civil structures and infrastructure subject to continuous loads ([Hagen
68 and Tvedt 1991](#); [Ferrante et al. 2005](#); [Li et al. 2005](#); [Pillai and Veena 2006](#)). For exam-
69 ple, [Li et al. \(2005\)](#) developed a method for reliability analysis considering a non-stationary
70 Gaussian vector process. [Beck and Melchers \(2005\)](#) investigated the error introduced in the
71 calculation of the upcrossing rate in the presence of a random barrier. The load stochastic
72 process has been, for the most part, modeled as Gaussian in existing studies, which may
73 differ significantly from the realistic case since a Gaussian (normal) distribution may lead to
74 a non-positive value of the load effect, inconsistent with the physical-based properties. [Li](#)

75 [et al. \(2016a\)](#) developed a closed-form solution to the “first passage probability” considering
76 a non-stationary lognormal distribution. The Nataf transformation method can be used to
77 convert a nonnormal stochastic process into a normal one (e.g., [Zheng and Ellingwood 1998](#)),
78 which is applicable for cases where the load process follows an arbitrary distribution (e.g.,
79 a Weibull or Extreme Type I distribution, as has also been widely used in existing studies
80 ([Melchers 1999](#); [Tang and Ang 2007](#))). However, existing approaches for reliability assess-
81 ment considering the temporal autocorrelation in the load process are complicated, with
82 which the application of reliability assessment in practical use may be difficult. A model of
83 load autocorrelation is essentially desirable to enable feasible compatibility to practical cases
84 and also an efficient approach of structural reliability assessment.

85 This paper develops a method for structural time-dependent reliability analysis, where,
86 in order to achieve a simple and efficient solution to the structural reliability, a new power
87 spectral density function of the load process is proposed, containing two parameters that
88 can be calibrated in an explicit form. Illustrative examples are presented to demonstrate the
89 applicability of the proposed method and to investigate the role of stochastic load process in
90 structural reliability. The difference between the reliabilities associated with a discrete load
91 process and a continuous one is also discussed.

92 **STOCHASTIC PROCESS-BASED RELIABILITY ASSESSMENT**

93 **Gaussian process of loads**

94 The time-dependent reliability based on the stochastic process theory has been well
95 documented in the literature ([Grigoriu 1984](#); [Engelund et al. 1995](#); [Li et al. 2016b](#)) and
96 is introduced briefly in this section. Consider the case where the load process in Eq. (1) is
97 Gaussian. Let

$$Z(t) = \mathcal{R}(t) - \mathcal{S}(t) = \Omega(t) - X(t) \quad (4)$$

98 where $\Omega(t) = \mathcal{R}(t) - \mathbb{E}[\mathcal{S}(t)]$ and $X(t) = \mathcal{S}(t) - \mathbb{E}[\mathcal{S}(t)]$, with \mathbb{E} denoting the mean value of the
99 random variable in the bracket. With this, $X(t)$ in Eq. (4) is a stationary Gaussian process

100 with a mean value of 0 and a standard deviation of $\sigma_X = \sigma_S$, where σ_S is the standard
 101 deviation of $\mathcal{S}(t)$. Fig. 2 presents an illustration of the upcrossing rate-based reliability
 102 problem. The positive upcrossing rate of $X(t)$ relative to $\Omega(t)$ at time t , $\nu^+(t)$, is estimated
 103 by (e.g., [Lutes and Sarkani 2004](#))

$$\begin{aligned} \lim_{dt \rightarrow 0} \nu^+(t)dt &= \Pr \left\{ \Omega(t) > X(t) \cap \Omega(t+dt) < X(t+dt) \right\} \\ &= \Pr \left\{ \Omega(t+dt) - \dot{X}(t)dt < X(t) < \Omega(t) \right\} \\ &= \int_{\dot{\Omega}(t)}^{\infty} [\dot{X}(t) - \dot{\Omega}(t)] f_{X\dot{X}} [\Omega(t), \dot{X}(t)] d\dot{X}(t)dt \end{aligned} \quad (5)$$

104 where \dot{X} (or $\dot{\Omega}$) denotes the derivative of X (or Ω). Rearranging Eq. (5) gives

$$\nu^+(t) = \int_{\dot{\Omega}(t)}^{\infty} (\dot{X} - \dot{\Omega}) f_{X\dot{X}} (\Omega, \dot{X}) d\dot{X} \quad (6)$$

105 Since $X(t)$ is a 0-mean stationary Gaussian process, $X(t)$ and $\dot{X}(t)$ are mutually independent,
 106 with which one has

$$f_{X\dot{X}}(x, \dot{x}) = \frac{1}{2\pi\sigma_X\sigma_{\dot{X}}} \exp \left\{ -\frac{1}{2} \left(\frac{x^2}{\sigma_X^2} + \frac{\dot{x}^2}{\sigma_{\dot{X}}^2} \right) \right\} \quad (7)$$

107 where $\sigma_{\dot{X}}$ is the standard deviation of $\dot{X}(t)$. Substituting Eq. (7) into Eq. (6) gives

$$\nu^+(t) = \frac{1}{2\pi\sigma_X} \exp \left[-\frac{\Omega^2(t)}{2\sigma_X^2} \right] \cdot \left\{ \sigma_{\dot{X}} \exp \left(-\frac{\dot{\Omega}^2(t)}{2\sigma_{\dot{X}}^2} \right) - \sqrt{2\pi}\dot{\Omega}(t) \left[1 - \Phi \left(\frac{\dot{\Omega}(t)}{\sigma_{\dot{X}}} \right) \right] \right\} \quad (8)$$

108 where $\Phi(\cdot)$ is the CDF of standard normal distribution. Assuming that the upcrossings of
 109 $X(t)$ to $\Omega(t)$ are temporally independent and are rare (e.g., at most one upcrossing may occur
 110 during a short time interval), the Poisson point process can be used to model the occurrence
 111 of the upcrossings. Let N_T denote the number of upcrossings during time interval $[0, T]$, and
 112 it follows,

$$\Pr(N_T = i) = \frac{1}{i!} \left\{ \int_0^T \nu^+(t)dt \right\}^i \exp \left\{ -\int_0^T \nu^+(t)dt \right\} \quad (9)$$

113 for $i = 0, 1, 2, \dots$. Further, the structural reliability during $[0, T]$ is the probability of $N_T = 0$,
 114 i.e.,

$$\mathbb{L}(T) = [1 - \mathbb{P}(0)] \exp \left\{ - \int_0^T \nu^+(t) dt \right\} \quad (10)$$

115 where $\mathbb{P}(0)$ is the failure probability at initial time. Specifically, as $\mathbb{P}(0)$ is typically small
 116 enough, one has ([Engelund et al. 1995](#); [Melchers 1999](#))

$$\mathbb{L}(T) = \exp \left\{ - \int_0^T \nu^+(t) dt \right\} \quad (11)$$

117 Eq. (11) presents the time-dependent reliability for a reference of T years. The derivation of
 118 $\nu^+(t)$ in Eq. (11) has been based on the assumption of a Gaussian process of loads. This may
 119 lead to a significantly biased estimate of structural reliability in many cases where the load
 120 effect follows a non-Gaussian distribution such as a lognormal, Weibull or Extreme Type I
 121 distribution. A more generalized case will be discussed subsequently, where the load process
 122 may follow an arbitrary distribution. Finally, it is noticed that the resistance deterioration
 123 process is assumed to be deterministic in this paper; for cases where the uncertainties as-
 124 sociated with the deterioration are non-negligible and shall be taken into account, one may
 125 use the total probability theorem to obtain the “expectation” of the structural reliability
 126 ([Rackwitz 2001](#)).

127 **Arbitrary stochastic process of loads**

128 In this section, the time-dependent reliability in the presence of an arbitrary stochastic
 129 process of loads is discussed. First, reconsider the time-variant limit state function $Z(t)$ in
 130 Eq. (4). Note that

$$\Pr[Z(t) > 0] = \Pr[\mathcal{R}(t) - \mathcal{S}(t) > 0] = \Pr \left\{ \Phi^{-1} \left[F_{S(t)}(\mathcal{R}(t)) \right] - \mathcal{Q}(t) > 0 \right\} \quad (12)$$

131 where $\mathcal{Q}(t) = \Phi^{-1} \left[F_{S(t)}(\mathcal{S}(t)) \right]$. With this, the term $\mathcal{Q}(t)$ is assigned as a standard Gaussian
 132 process, and further an “equivalent resistance” is defined as $\mathcal{R}^*(t) = \Phi^{-1} \left[F_{S(t)}(\mathcal{R}(t)) \right]$. In

133 such a way, the time-dependent reliability analysis is transformed into solving a standard
 134 “first passage probability” problem. That is, Eqs. (8) and (11) apply in the presence of the
 135 “equivalent” resistance and load.

136 A key step herein is to find the correlation in $\mathcal{Q}(t)$ provided that the correlation in $\mathcal{S}(t)$
 137 is known. Suppose that the correlation coefficient between $\mathcal{S}_i = \mathcal{S}(t_i)$ and $\mathcal{S}_j = \mathcal{S}(t_j)$ is ρ_{ij} ,
 138 and the correlation coefficient between the corresponding $\mathcal{Q}_i = \mathcal{Q}(t_i)$ and $\mathcal{Q}_j = \mathcal{Q}(t_j)$ is ρ'_{ij} .
 139 The relationship between ρ_{ij} and ρ'_{ij} can be determined by (Liu and Der Kiureghian 1986;
 140 Melchers 1999)

$$\rho_{ij} = \int_{-\infty}^{\infty} \int_{-\infty}^{\infty} \Theta_1 \Theta_2 \cdot \Psi(y_1, y_2; \rho'_{ij}) dy_2 dy_1 \quad (13)$$

in which Θ_1 , Θ_2 and Ψ are given by

$$\Theta_1 = \frac{F_{\mathcal{S}_i}^{-1}(\Phi(y_1)) - \mathbb{E}(\mathcal{S}_i)}{\sqrt{\mathbb{V}(\mathcal{S}_i)}}; \quad (14a)$$

$$\Theta_2 = \frac{F_{\mathcal{S}_j}^{-1}(\Phi(y_2)) - \mathbb{E}(\mathcal{S}_j)}{\sqrt{\mathbb{V}(\mathcal{S}_j)}}; \quad (14b)$$

$$\Psi(y_1, y_2; \rho'_{ij}) = \frac{1}{2\pi\sqrt{1 - \rho'^2_{ij}}} \exp\left\{ \frac{y_1^2 - 2\rho'_{ij}y_1y_2 + y_2^2}{2(1 - \rho'^2_{ij})} \right\} \quad (14c)$$

141 where $F_{\mathcal{S}_i}^{-1}$ is the inverse of the CDF of \mathcal{S}_i , and $\mathbb{V}(\cdot)$ denote the variance of the random variable
 142 in the bracket. Equations. (13) and (14) are the key component of the Nataf transformation
 143 (i.e., the transformation from $\mathcal{S}(t)$ to $\mathcal{Q}(t)$ herein) addressing the autocorrelation structure
 144 of the Gaussian process $\mathcal{Q}(t)$. Eq. (13) indicates that ρ'_{ij} depends on the COV (coefficient
 145 of variation) of \mathcal{S}_i and \mathcal{S}_j only if ρ_{ij} is given.

146 It is noticed that the method of “equivalent” resistance and load is a generalized form of
 147 the “translation process” method developed by Grigoriu (1984), where a constant barrier level
 148 was considered. Moreover, Grigoriu (1984) also suggested that the use of a Nataf transform
 149 method results in a negligible error in the estimate of upcrossing rate for many common
 150 distribution types such as Weibull, Extreme Type I, lognormal and Gamma, implying the
 151 feasibility of the Nataf transformation-based method in dealing with practical reliability

152 problems with a non-Gaussian load process. [Kim and Shields \(2015\)](#) presented a further
 153 development on Grigoriu's translation processes for strongly non-Gaussian processes, where
 154 the transformation was realized with an iteration-based simulation approach that considers
 155 the autocorrelation function of the stochastic process. However, a simulation-based method
 156 may limit the applicability of reliability assessment in practical use due to the relatively low
 157 efficiency compared with a closed-form solution.

158 RELIABILITY WITH A CONTINUOUS OR A DISCRETE LOAD PROCESS

159 Recall that the time-dependent reliability problem has been addressed in Eqs. (2) and
 160 (11), respectively. The former considers a discrete load process where only the significant
 161 load events that may impair the structural safety directly are incorporated, while the later
 162 is derived based on a continuous load process. The difference between the two types of load
 163 model is discussed in this section.

164 First, consider the CDF of $\max\{X(t)\}$ within a time duration of Δ , $F_{X_{\max|\Delta}}$, where
 165 $X(t) = \mathcal{S}(t) - \mathbb{E}[\mathcal{S}(t)]$ is the normalized load process (c.f. Eq. (4)). In the presence of a
 166 continuous Gaussian load process, with Eqs. (8) and (11), let $\Omega(t) = x$ and $\dot{\Omega}(t) = 0$, which
 167 corresponds to the case of a constant boundary, one has

$$F_{X_{\max|\Delta}}(x) = \exp \left\{ -\frac{\sigma_{\dot{X}}}{2\pi\sigma_X} \exp \left(-\frac{x^2}{2\sigma_X^2} \right) \Delta \right\} \quad (15)$$

168 Further, as Δ is small enough ([Newland 1993](#))

$$F_{X_{\max|\Delta}}(x) \approx 1 - \frac{\sigma_{\dot{X}}\Delta}{2\pi\sigma_X} \exp \left(-\frac{x^2}{2\sigma_X^2} \right) \quad (16)$$

169 which yields a Rayleigh distribution. Eq. (16) suggests that the maximum load effect within
 170 a time interval that is sufficiently short necessarily follows a Rayleigh distribution, if the
 171 continuous load process is Gaussian. For a discrete load process, e.g., a Poisson process,

172 however, the distribution of $\max\{X(t)\}$ within a short time interval of Δ is given by

$$F_{X_{\max|\Delta}}(x) = 1 - \lambda\Delta \cdot (1 - F_S(x)) \quad (17)$$

173 where λ is the mean occurrence rate of the Poisson process, and F_S is the CDF of load
 174 magnitude conditional on the occurrence of one load event. Eq. (17) indicates that the CDF
 175 of maximum load is eventually dependent on F_S , and thus may vary for different distributions
 176 of each load event. Letting the two CDFs of maximum load in Eqs. (16) and (17) be equal
 177 yields

$$F_S(x) = 1 - \frac{\sigma_{\dot{X}}}{2\pi\lambda\sigma_X} \exp\left(-\frac{x^2}{2\sigma_X^2}\right) \quad (18)$$

178 Eq. (18) suggests that if a continuous Gaussian process is transformed to a discrete one,
 179 the CDF of the load effect conditional on the occurrence of one load event simply follows a
 180 Rayleigh distribution.

181 For the more generalized case of a non-Gaussian load process, $X(t)$ can be converted into
 182 a Gaussian process $\mathcal{Q}(t)$, as discussed before. With this, for a reference period of Δ , the
 183 CDF of $\max\{X(t)\}$ is given by

$$F_{X_{\max|\Delta}}(x) = \Pr \left\{ \bigcap_{0 \leq t \leq \Delta} \left(\Phi^{-1}[F_S(\mathcal{S}(t))] < \Phi^{-1}(F_S(x)) \right) \right\} \quad (19)$$

184 Let $x^* = \Phi^{-1}(F_S(x))$, and Eq. (19) becomes

$$\begin{aligned} F_{X_{\max|\Delta}}(x) &= \exp \left\{ -\frac{\sigma_{\dot{\mathcal{Q}}}\Delta}{2\pi} \exp \left(-\frac{x^{*2}}{2} \right) \right\} \\ &\approx 1 - \frac{\sigma_{\dot{\mathcal{Q}}}\Delta}{2\pi} \exp \left(-\frac{x^{*2}}{2} \right) \\ &= 1 - \frac{\sigma_{\dot{\mathcal{Q}}}\Delta}{2\pi} \exp \left\{ -\frac{[\Phi^{-1}(F_S(x))]^2}{2} \right\} \end{aligned} \quad (20)$$

185 It should be noted that Eq. (20) is only valid when x is large enough. Eq. (20) implies
 186 that when the load process is non-Gaussian, the maximum load effect within a time interval

187 does not necessarily follow a Rayleigh distribution. The distribution type in Eq. (20) is the
 188 original development of the present paper and is referred to as ‘‘Pseudo-Rayleigh distribution’’
 189 by the authors. Nonetheless, the distribution type of $\max\{X(t)\}$ is determined if $X(t)$ is
 190 continuous, which again differs from the case of a discrete load process.

191 Next, the difference between the reliabilities associated with a discrete load process and
 192 a continuous one is discussed. For simplicity, the load process is assumed to be Gaussian.
 193 With a discrete load process, the time-dependent reliability within $[0, T]$ is estimated by

$$\mathbb{L}_d(T) = \Pr \left[\bigcap_{0 < t \leq T} (\Omega(t) - X_{\max} > 0) \right] = \exp \left[-\frac{\sigma_{\dot{X}}}{2\pi\sigma_X} \int_0^T \exp \left(-\frac{\Omega^2(t)}{2\sigma_X^2} \right) dt \right] \quad (21)$$

194 which takes a similar form of Eq. (11) with a different upcrossing rate $\nu^+(t)$ in Eq. (8). In
 195 fact, Eq. (8) can be rewritten as

$$\nu^+(t) = \frac{\sigma_{\dot{X}}}{2\pi\sigma_X} \exp \left[-\frac{\Omega^2(t)}{2\sigma_X^2} \right] \cdot h(z) \quad (22)$$

196 where

$$h(z) = \exp \left(-\frac{z^2}{2} \right) - \sqrt{2\pi}z [1 - \Phi(z)] \quad (23)$$

197 with $z = z(t) = \frac{\dot{\Omega}(t)}{\sigma_X}$. Intuitively, for a constant barrier level, $z = 0$ since $\dot{\Omega}(t) = 0$, with
 198 which $h(z) = 1$, consistent with the results in [Gomes and Vickery \(1977\)](#).

199 By noting that z is typically negative as $\dot{\Omega}(t) < 0$ and that $h(z)$ is a monotonically
 200 decreasing function of z , $h(z) \geq h(0) = 1$ for $\forall z < 0$. For simplicity, Eq. (22) is rewritten as
 201 $\nu^+(t) = \nu_0^+(t) \cdot h(z)$. According to Eq. (11), the time-dependent reliability with a continuous
 202 load process is given by

$$\mathbb{L}(T) = \exp \left\{ -\int_0^T \nu^+(t) dt \right\} = \exp \left\{ -\int_0^T \nu_0^+(t) h(z) dt \right\} \quad (24)$$

203 With the mean value theorem for integrals (e.g., [Comenetz 2002](#)), there exists a real number

204 $z_0 \in [\min_{t=0}^T z(t), \max_{t=0}^T z(t)]$ such that

$$\mathbb{L}(T) = \exp \left\{ -h(z_0) \cdot \int_0^T \nu_0^+(t) dt \right\} = [\mathbb{L}_d(T)]^{h(z_0)} \leq \mathbb{L}_d(T) \quad (25)$$

205 Thus, it can be concluded that the choice of a discrete load model overestimates the structural
 206 safety or equivalently, underestimates the failure probability, if the realistic load process is
 207 continuous. In fact, with Eq. (25), since $\mathbb{P}_d(T) = 1 - \mathbb{L}_d(T)$ is typically small enough for
 208 well-designed structures, one has

$$\mathbb{P}(T) = 1 - [\mathbb{L}_d(T)]^{h(z_0)} = 1 - [1 - \mathbb{P}_d(T)]^{h(z_0)} \approx h(z_0) \cdot \mathbb{P}_d(T) \quad (26)$$

209 which implies that the failure probability is underestimated by a factor of $\frac{1}{h(z_0)}$ if the con-
 210 tinuous load process is modeled as a discrete one. It is noticed, however, that the difference
 211 between $\mathbb{P}(T)$ and $\mathbb{P}_d(T)$ may be fairly small for many practical cases where $h(z_0)$ is close
 212 to 1.0; this point will be further discussed in the following.

213 A NEW POWER SPECTRAL DENSITY FUNCTION

214 In stochastic process theory based time-dependent reliability analysis, one of the crucial
 215 ingredients is the modeling of the autocorrelation in the load process. For a stationary
 216 process, say, $X(t)$, the autocorrelation is only dependent on the time separation τ but not the
 217 absolute time. With this, the autocorrelation in $X(t)$ is defined as $R(\tau) = \mathbb{E}[X(t)X(t+\tau)] =$
 218 $R(-\tau)$ (Newland 1993). An illustrative example is presented in Fig. 3, which shows the
 219 dependence of autocorrelation in the hurricane load process on the time interval between
 220 two successful hurricane events (Ellingwood and Lee 2016). The autocorrelation decreases
 221 sharply at the early stage where τ is relatively small, and converges to zero latter with a
 222 fluctuation along the horizontal axis. Such an autocorrelation function also applies to many
 223 other types of external loads which are affected by common underlying causes (Wang and
 224 Zhang 2018).

The spectral density function of $S(\omega)$, which is a Fourier transform of $R(\tau)$, also provides

a tool to describe the statistical characteristics of $X(t)$. Mathematically, one has

$$R_X(\tau) = 2 \int_0^\infty S(\omega) \cos(\omega\tau) d\omega \quad (27a)$$

$$\sigma_{\dot{X}}^2 = R_{\dot{X}}(0) = -\frac{d^2 R_X(0)}{d\tau^2} = 2 \int_0^\infty \omega^2 S(\omega) d\omega \quad (27b)$$

Eq. (27b) implies that a spectral density function, $S(\omega)$, consequently gives an estimate of the standard deviation of $\dot{X}(t)$. However, since an improper integral is involved in Eq. (27b), an arbitrary form of $S(\omega)$ does not necessarily lead to a converged form of $\sigma_{\dot{X}}$. For example, if $R(\tau)$ takes the form of $R(\tau) = \sigma_X^2 \exp(-k\tau)$ (c.f. Eq. (3)), where σ_X is the standard deviation of $X(t)$, it follows (e.g., Zheng and Ellingwood 1998)

$$S(\omega) = \frac{1}{\pi} \int_0^\infty R(\tau) \cos(\tau\omega) d\tau = \frac{k\sigma_X^2}{\pi(k^2 + \omega^2)} \quad (28)$$

with which Eq. (27b) does not converge. Furthermore, even for some spectral density functions that result in a converged $\sigma_{\dot{X}}$, the integral operation in Eq. (27b) may be inefficient when used in the structural reliability assessment in Eq. (11) (that is, a two-fold integral will be involved in Eq. (11) if substituting Eqs. (8) and (27b) into Eq. (11)), especially for use in practical engineering.

In an attempt to achieve a simple and convergent form of Eq. (27b), a new power spectral density function is developed in this section, which takes the form of

$$S(\omega) = \frac{a}{\omega^6 + b}, \quad -\infty < \omega < +\infty \quad (29)$$

where a and b are two constants. It can be seen that Eq. (29) satisfies the basic properties of a power spectral density function: it's an even function of ω (i.e., $S(-\omega) = S(\omega)$) and positive (this is satisfied by noting that both a and b are positive values, see Eq. (35) below).

With the proposed spectral density function in Eq. (29), according to Eq. (27), it follows

$$R(\tau) = R(\tau, b) = 2a \cdot \int_0^\infty \frac{1}{\omega^6 + b} \cos(\omega\tau) d\omega \quad (30a)$$

$$\sigma_X^2 = R(0, b) = 2a \cdot \int_0^\infty \frac{1}{\omega^6 + b} d\omega = \frac{2a\pi}{3b^{5/6}} \quad (30b)$$

240 The integral operation involved in Eq. (30a) can be solved in a closed form. To begin with,
 241 one has

$$R(1, b) = \frac{2a\pi}{12b^{5/6}} \exp\left(-\frac{b^{1/6}}{2}\right) \cdot \left[2 \exp\left(-\frac{b^{1/6}}{2}\right) + 4 \cos\left(\frac{\sqrt{3}}{2}b^{1/6} - \frac{\pi}{3}\right)\right] \quad (31)$$

242 Further, it is easy to find that

$$R(\tau, b) = \tau^5 \cdot R(1, b\tau^6) \quad (32)$$

243 As such, Eq. (30) provides a straightforward approach to find a and b in the density function
 244 $S(\omega)$, provided that the autocorrelation function in the load process is known. It is noticed
 245 that while the autocorrelation function in Eq. (32) has been derived directly based on Eq. (29)
 246 rather than from a physics-based case, Eq. (32) nevertheless is feasible to capture different
 247 dependence scenarios of load autocorrelation on the time separation that decreases sharply at
 248 the early stage and subsequently fluctuates along the time axis with a decreasing magnitude.
 249 This fact is guaranteed by noting that in Eq. (32), the magnitude of $R(\tau, b)$ is controlled
 250 by the term $\exp\left(-\frac{b^{1/6}\tau}{2}\right)$, which is a monotonically decreasing function of τ with a given b ,
 251 while the fluctuation of $R(\tau, b)$ is posed by the term $2 \exp\left(-\frac{b^{1/6}\tau}{2}\right) + 4 \cos\left(\frac{\sqrt{3}}{2}b^{1/6}\tau - \frac{\pi}{3}\right)$.

252 For illustration purpose, Fig. 4 shows the dependence of $R(\tau)$ on the time separation τ for
 253 $b = 30, 60$ and 90 , respectively, assuming $a = 1$ for all the three cases. The autocorrelation
 254 decreases sharply at the early stage where τ is relatively small, and converges to zero soon
 255 with a fluctuation along the horizontal axis. The overall trends in Fig. 4 coincide well with
 256 that in Fig. 3. Moreover, it is seen that the different values of b result in different shapes of

257 the autocorrelation function, indicating that the proposed spectral density function enables
 258 freedom for different depending scenarios of $R(\tau)$ on the time separation τ .

259 With the autocorrelation in $X(t)$ addressed, one can further find the correlation coefficient
 260 in $X(t)$, $\rho(\tau)$, by $\rho(\tau) = R(\tau)/\sigma_X^2$. For instance, for a unit time separation of $\tau = 1$, one has

261

$$\rho(1, b) = \frac{1}{4} \exp\left(-\frac{b^{1/6}}{2}\right) \cdot \left[2 \exp\left(-\frac{b^{1/6}}{2}\right) + 4 \cos\left(\frac{\sqrt{3}}{2}b^{1/6} - \frac{\pi}{3}\right)\right] \quad (33)$$

262 Mathematically, it is easy to see that $\lim_{b \rightarrow 0} \rho(1, b) = 1$ and $\lim_{b \rightarrow \infty} \rho(1, b) = 0$. Eq. (33) can
 263 be simply extended to other values of τ by noting that

$$\rho(\tau) = \rho(\tau, b) = \frac{R(\tau, b)}{\sigma_X^2} = \frac{\tau^5 \cdot R(1, b\tau^6)}{\sigma_X^2} \quad (34)$$

264 Further, with $S(\omega)$ taking the form of Eq. (29), it follows

$$\sigma_X^2 = 2a \cdot \int_0^\infty \frac{\omega^2}{\omega^6 + b} d\omega = \frac{\pi a}{3\sqrt{b}} \quad (35)$$

265 It can be seen from Eq. (35) that both a and b are positive real numbers due to the fact that
 266 σ_X^2 is a positive real number. Furthermore, with Eq. (35), it is easy to see that Eq. (8) has a
 267 simple form with only fundamental algebras involved, which is beneficial for the application of
 268 structural reliability assessment when substituting Eq. (8) into Eq. (11). The applicability
 269 of the proposed power density function will be demonstrated in the next section. It is
 270 emphasized, finally, that for the case where the load process is non-Gaussian, the proposed
 271 density function also applies, if both the resistance and load effect are converted to the
 272 “equivalent” ones respectively, as discussed above.

273 NUMERICAL EXAMPLE

274 In this section, an illustrative example is presented to demonstrate the applicability of the
 275 proposed power spectral density function in structural time-dependent reliability assessment,
 276 and to investigate the role of load autocorrelation in structural safety.

277 Consider a structure subjected to the joint effect of both a dead load \mathcal{D} and a continuous
278 lateral load \mathcal{H} (due to, e.g., the lateral earth pressure (Clayton et al. 2014)). Table 1 presents
279 the probability distribution of the resistance and loads, with a load combination as follows
280 (ASCE standard 7, ASCE 2002),

$$0.75\mathcal{R}_n = 0.9\mathcal{D}_n + 1.6\mathcal{H}_n \quad (36)$$

281 where \mathcal{R}_n is the nominal resistance, \mathcal{D}_n is the nominal dead load, and \mathcal{H}_n is the nominal
282 lateral load. Assume that $\mathcal{D}_n = \mathcal{H}_n$.

283 The initial resistance and dead load are modeled as deterministic, due to the fact that
284 the randomness associated with the live loads contributes to the majority of the overall
285 uncertainties for most engineered structures (e.g., Ellingwood et al. 1982; Ellingwood and
286 Hwang 1985). The initial resistance has a value of 1.1 times the nominal resistance reflecting
287 the modeling bias. The dead load is approximated by the nominal value which coincides
288 well with many *in-situ* surveys. The live load in Table 1 in fact represents the “arbitrary
289 point-in-time” load having a value that would be measured if the load process were to be
290 sampled at some specific time instants.

291 A reference period of 50 years (i.e., T is up to 50 years) is considered in the following
292 analysis. Moreover, taking into account the operational environmental factors that are re-
293 sponsible for the deterioration of structural resistance (e.g., the corrosion of steel bars in RC
294 structures due to the ingress of Chloride in marine/coastal areas (Pang and Li 2016)), it
295 is assumed that the structural resistance degrades linearly by 20% over a reference period
296 of 50 years. The autocorrelation coefficient in the lateral load process is assumed to be 0.3
297 for a time separation of 1 year (i.e., $R(1 \text{ year}) = 0.3\sigma_H^2$, where σ_H is the standard deviation
298 of \mathcal{H}). It is emphasized that while a lognormal stochastic load process (that is, the load
299 process evaluated at an arbitrary time follows a lognormal distribution) is considered herein,
300 the method in this paper is also applicable for loads with other distribution types such as a

301 Weibull or Extreme Type I distribution (Melchers 1999; Tang and Ang 2007).

302 Note that the lateral load \mathcal{H} follows a lognormal distribution, and thus is transformed
 303 into a standard normal distribution \mathcal{H}^* by $F_H(\mathcal{H}) = \Phi(\mathcal{H}^*)$, where F_H is the CDF of \mathcal{H} .
 304 With this, according to Eq. (13), the autocorrelation coefficient in the process $\mathcal{H}^*(t)$ for a
 305 time separation of 1 year is found to be $\frac{\ln(1 + 0.3c_H^2)}{\ln(1 + c_H^2)} = 0.3241$, where c_H is the COV of \mathcal{H} .
 306 As such, with Eq. (30), the two parameters a and b can be found numerically as 18.1 and 78.7
 307 respectively for \mathcal{H}^* . Fig. 5 shows the autocorrelation coefficient in \mathcal{H}^* as a function of time
 308 difference τ , where an exponential decay model is also presented for comparison. It can be
 309 seen that with both types of correlation coefficient function, the autocorrelation in the load
 310 process diminishes rapidly for τ being up to three years. to have a similar shape overall.
 311 Moreover, in Fig. 5, the autocorrelation coefficient in $\mathcal{H}(t)$ assuming a Gaussian process
 312 of $\mathcal{H}(t)$ is also plotted, as well as an exponential law of the autocorrelation decay in the
 313 “assumed” normal $\mathcal{H}(t)$. The difference between the time-variation scenarios of correlation
 314 coefficient functions associated with \mathcal{H}^* and normal \mathcal{H} is negligible.

315 The spectral density function takes the form of Eq. (29), with which the autocorrelation
 316 coefficient in $\mathcal{H}^*(t)$ is modeled by Eq. (34). With the two parameters a and b obtained,
 317 one can simulate a sample sequence of $\mathcal{H}^*(t)$ and correspondingly, $\mathcal{H}(t)$. Since $\mathcal{H}^*(t)$ is a
 318 standard Gaussian process, one has (Newland 1993)

$$\mathcal{H}^*(t) \sim \sqrt{\frac{2}{N}} \cdot \sum_{j=1}^N \cos(\omega_j t + \theta_j) \quad (37)$$

319 where N is a sufficiently large integer, ω_j is a real random variable with a PDF of $S(\omega)$ (Note
 320 that the standard deviation of \mathcal{H}^* is 1.0, and thus $\int_{-\infty}^{\infty} S(\omega)d\omega = 1$), and θ_j is a random
 321 variable that is uniformly distributed in $[0, 2\pi]$. The simulation method for ω_j is discussed
 322 in Appendix I. Fig. 6 demonstrates sample sequences for $\mathcal{H}^*(t)$ and $\mathcal{H}(t)$ (normalized by
 323 \mathcal{H}_n), respectively. Such realizations in Fig. 6 provide a straightforward impression on the
 324 time-variation of the stochastic process with certain statistical characteristics.

325 Fig. 7(a) shows the time-dependent failure probabilities for reference periods up to 50
 326 years, assuming a mean lateral load of $0.4\mathcal{H}_n$, $0.5\mathcal{H}_n$ (as in Table 1) and $0.6\mathcal{H}_n$, respectively.
 327 A greater load magnitude leads to a higher probability of failure. For reference periods
 328 exceeding 10 years, the logarithmic failure probability increases approximately linearly with
 329 time, which is consistent with the observations in Li et al. (2015). For comparison purpose,
 330 Fig. 7(b) presents the time-dependent failure probabilities assuming a Gaussian process of
 331 loads. It can be seen from the comparison between Figs. 7(a) and (b) that the assumption of
 332 a Gaussian load process underestimates the failure probability compared with the lognormal
 333 load process. This observation can be explained by examining the upper tail behaviour of a
 334 normal distribution and a lognormal distribution, as shown in Fig. 8. With the same mean
 335 value and standard deviation, a lognormal distribution has a longer upper tail compared with
 336 a normal distribution, and thus results in a greater probability that the random variable
 337 exceeds a given threshold. Specifically, suppose that the structural failure probability is
 338 represented by $F(1.0\mathcal{H}_n)$, where F is the CDF of either a lognormal or a normal distribution
 339 in Fig. 8. For the case of $0.4\mathcal{H}_n$, the failure probability associated with a lognormal load is
 340 0.015, which is approximately 10 times of that associated with a normal distribution. This
 341 fact indicates that treating a non-Gaussian load process as Gaussian may result in significant
 342 error in the estimate of structural reliability.

343 In order to investigate the impact of load autocorrelation on structural time-dependent
 344 reliability, Fig. 9 presents the time-dependent failure probabilities for different cases of cor-
 345 relation coefficients in load: case (1) $\rho(1 \text{ year}) = 0.1$, case (2) $\rho(1 \text{ year}) = 0.3$ (the same as
 346 before) and case (3) $\rho(1 \text{ year}) = 0.5$. Correspondingly, the autocorrelation coefficients in
 347 \mathcal{H}^* are 0.1107, 0.3241 and 0.5278 for a time separation of 1 year. Further, with Eq. (33),
 348 the parameter b is found as 371.1, 78.7 and 16.4 respectively for the three cases. In Fig. 9,
 349 the failure probability increases exponentially with T for reference periods exceeding 10
 350 years, which is consistent with the observation from Fig. 7(a). Moreover, Fig. 9 suggests
 351 that a stronger autocorrelation in loads leads to a smaller failure probability. This can be

352 explained by considering an extreme case where the structural survival is represented by
353 $S_1 < r \cap S_2 < r$, where r is the resistance (a deterministic value), S_1 and S_2 are two iden-
354 tically distributed loads with a CDF of F . For the case of fully correlated S_1 and S_2 , the
355 failure probability is simply $1 - F(r)$, which is greater than that associated with independent
356 S_1 and S_2 (i.e., $1 - F^2(r)$). Fig. 9 on one hand implies the importance of identifying the
357 load autocorrelation in an accurate estimate of structural reliability, and on the other hand
358 suggests that for cases where only insufficient load information is available, the assumption
359 of a weak autocorrelation in loads leads to a relatively conservative estimate of structural
360 reliability.

361 By noting that the load process follows a lognormal distribution, as summarized in Ta-
362 ble 1, the CDF of maximum load effect within a reference period of Δ can be found through
363 Eq. (20). Fig. 10 plots the CDFs of maximum load for cases of $\rho(1 \text{ year}) = 0.1, 0.3$ and 0.5 ,
364 respectively. A stronger load autocorrelation leads to a shorter upper tail of the CDF, and
365 subsequently results in a smaller exceeding probability given a predefined threshold. This
366 observation is consistent with the one from Fig. 9 that a greater load autocorrelation leads
367 to a smaller failure probability.

368 Finally, the difference between the failure probabilities associated with a discrete load
369 process and a continuous one is discussed. The failure probabilities are calculated with
370 Eqs. (21) and (26), respectively. For the three cases in Fig. 7(a), the difference between
371 $\mathbb{P}(T)$ and $\mathbb{P}_d(T)$ is found to be negligible. For instance, for a reference period of 50 years,
372 if the mean value of $\mathcal{H}(t)$ is $0.5\mathcal{H}_n$, then $\mathbb{P}(T)$ and $\mathbb{P}_d(T)$ are equal to 0.036 and 0.035,
373 respectively (with a difference of less than 2%). This small difference can be explained as
374 follows. Consider a Gaussian load process, with which the term z in Eq. (23) is rewritten as
375 follows,

$$z = \frac{\dot{\Omega}(t)}{\sigma_{\dot{X}}} = \frac{\dot{\Omega}(t)}{\sqrt{\frac{\pi a}{3\sqrt{b}}}} = \frac{\sqrt{2}\dot{\Omega}(t)}{\sigma_X b^{1/6}} \quad (38)$$

376 With the structural configuration in Table 1, for the typical cases where $\rho(1 \text{ year}) \leq 0.8$

377 (correspondingly, $b \geq 0.73$ according to Eq. (33)),

$$0 > z \geq \frac{-\sqrt{2} \cdot 0.2/50 \cdot \left(1.1 \cdot \frac{0.9\mathcal{D}_n + 1.6\mathcal{H}_n}{0.75}\right)}{0.5 \cdot 0.5\mathcal{H}_n \cdot 0.73^{1/6}} = -0.0874 \quad (39)$$

378 with which $\frac{1}{h(z_0)} \in [0.8981, 1]$. This fact implies that the difference between $\mathbb{P}(T)$ and $\mathbb{P}_d(T)$
379 has a maximum of approximately 10%. In fact, even for an extreme case where the resistance
380 degrades severely by 50% over a reference period of 50 years, the maximum difference between
381 the two failure probabilities is about 20%. As a result, it can be concluded that a continuous
382 load process can be reasonably modeled by a discrete process where only significant load
383 events are considered.

384 CONCLUSIONS

385 This paper has proposed a method to estimate the structural time-dependent reliability
386 in the presence of a new power spectral density function, which yields a simple and efficient
387 solution to the structural reliability. Illustrative examples are presented to demonstrate the
388 applicability of the proposed method. The following conclusions can be drawn from this
389 paper.

- 390 1. The structural time-dependent reliability analysis in the presence of a non-Gaussian
391 load process can be transformed into a standard “first passage probability” problem
392 by introducing an “equivalent” load. Provided that the autocorrelation in the load
393 process is known, the correlation coefficient function in the “equivalent” load process
394 can be uniquely determined.
- 395 2. Some types of power spectral density function of a stochastic process may result in
396 a non-convergent estimate of the standard deviation of the process’s derivative, and
397 thus cannot be used in reliability assessment directly (c.f. Eqs. (8) and (11)). The
398 proposed spectral density function as in Eq. (29), however, enables an analytical
399 estimate of the stochastic process’s characteristics, and further yields a closed-form
400 formula of structural time-dependent reliability.

- 401 3. If the load process is non-Gaussian, simply assuming a Gaussian process for loads may
402 lead to a significantly biased estimate of structural reliability. This fact indicates the
403 importance of properly addressing the distribution type of the load process.
- 404 4. A stronger load autocorrelation leads to a smaller failure probability. For cases where
405 the load information is insufficient, the assumption of a weak autocorrelation in loads
406 results in a relatively conservative estimate of structural reliability.
- 407 5. The impact of choosing a continuous or a discrete load model on structural reliability
408 is compared. The former leads to a specific distribution type (not necessarily Rayleigh
409 if the load process is non-Gaussian) of maximum load effect during a time interval of
410 interest. The assumption of a discrete stochastic process for loads overestimates the
411 structural safety compared with that associated with a continuous load model. The
412 difference is, however, negligible for most engineering cases, and thus the two methods
413 of modeling load process can be used exchangeably for the purpose of structural safety
414 assessment.

415 **APPENDIX I. ON THE SAMPLING OF A RANDOM VARIABLE WITH A KNOWN**
 416 **PDF**

417 In this section, the sampling of a random variable with a known PDF is discussed. The
 418 rejection method can be used to sample a random variable with a known PDF but follows
 419 an irregular distribution (Ross 2014).

420 First, consider a random variable X with a standard deviation of σ_X and a PDF of
 421 $f_X(x) = \frac{a_0}{x^6+b} = \frac{S(x)}{\sigma_X^2}$, where $S(x)$ is as in Eq. (29), and $a_0 = \frac{a}{\sigma_X^2}$. Clearly, one can show
 422 that $\int_{-\infty}^{\infty} f(x)dx = \int_{-\infty}^{\infty} \frac{S(x)}{\sigma_X^2}dx = 1$. For further derivation, an auxiliary random variable Y
 423 is introduced, which has a PDF of $f_Y(y) = \frac{\sqrt{b}/\pi}{y^2+b}$. The CDF of Y is $F_Y(y) = \int_{-\infty}^y \frac{\sqrt{b}/\pi}{z^2+b}dz =$
 424 $\frac{1}{\pi} \left(\arctan \left(\frac{y}{\sqrt{b}} \right) + \frac{\pi}{2} \right)$. Mathematically, it can be proven that

$$S(y) = \frac{a_0}{y^6 + b} \leq \frac{a_0(b+1)\pi}{b^{1.5}} \cdot f_Y(y) \quad (40)$$

425 With this, the procedure of sampling a realization x for X is as follows,

- 426 • Simulate two random numbers u_1 and u_2 that are uniformly distributed in $[0, 1]$.
- 427 • Set $y = \sqrt{b} \tan \left(u_1\pi - \frac{\pi}{2} \right)$.
- 428 • If $u_2 \leq \frac{S(y)}{\frac{a_0(b+1)\pi}{b^{1.5}} \cdot f_Y(y)}$, then set $x = y$; otherwise return to step 1 (i.e. re-sample u_1 and
 429 u_2).

430 This procedure has been used in the sampling of $\mathcal{H}^*(t)$ and $\mathcal{H}(t)$ in Fig. 6.

431 **ACKNOWLEDGEMENTS**

432 The research described in this paper was supported by the Faculty of Engineering and
 433 IT PhD Research Scholarship (SC1911) from the University of Sydney. This support is
 434 gratefully acknowledged. The authors would like to acknowledge the thoughtful suggestions
 435 of two anonymous reviewers, which substantially improved the present paper.

436 **REFERENCES**

437 Akiyama, M. and Frangopol, D. M. (2014). “Long-term seismic performance of rc structures
438 in an aggressive environment: Emphasis on bridge piers.” *Structure and Infrastructure*
439 *Engineering*, 10(7), 865–879.

440 ASCE (2002). *Minimum design loads for buildings and other structures*. American Society
441 of Civil Engineers.

442 Beck, A. T. and Melchers, R. E. (2005). “Barrier failure dominance in time variant reliability
443 analysis.” *Probabilistic engineering mechanics*, 20(1), 79–85.

444 Clayton, C. R., Woods, R. I., Bond, A. J., and Milititsky, J. (2014). *Earth pressure and*
445 *earth-retaining structures*. CRC Press.

446 Comenetz, M. (2002). *Calculus: the elements*. World Scientific Publishing Co Inc.

447 Ellingwood, B., MacGregor, J. G., Galambos, T. V., and Cornell, C. A. (1982). “Probability
448 based load criteria: load factors and load combinations.” *Journal of the Structural Division*,
449 108(5), 978–997.

450 Ellingwood, B. R. and Hwang, H. (1985). “Probabilistic descriptions of resistance of safety-
451 related structures in nuclear plants.” *Nuclear Engineering and Design*, 88(2), 169–178.

452 Ellingwood, B. R. and Lee, J. Y. (2016). “Life cycle performance goals for civil infrastructure:
453 intergenerational risk-informed decisions.” *Structure and Infrastructure Engineering*, 12(7),
454 822–829.

455 Engelund, S., Rackwitz, R., and Lange, C. (1995). “Approximations of first-passage times
456 for differentiable processes based on higher-order threshold crossings.” *Probabilistic Engi-*
457 *neering Mechanics*, 10(1), 53–60.

458 Enright, M. P. and Frangopol, D. M. (1998). “Service-life prediction of deteriorating concrete
459 bridges.” *Journal of Structural Engineering*, 124(3), 309–317.

460 Ferrante, F., Arwade, S., and Graham-Brady, L. (2005). “A translation model for non-
461 stationary, non-gaussian random processes.” *Probabilistic Engineering Mechanics*, 20(3),
462 215–228.

463 Gomes, L. and Vickery, B. (1977). “On the prediction of extreme wind speeds from the

parent distribution.” *Journal of Industrial Aerodynamics*, 2(1), 21–36.

Grigoriu, M. (1984). “Crossings of non-gaussian translation processes.” *Journal of Engineering Mechanics*, 110(4), 610–620.

Hagen, Ø. and Tvedt, L. (1991). “Vector process out-crossing as parallel system sensitivity measure.” *Journal of Engineering Mechanics*, 117(10), 2201–2220.

Kim, H. and Shields, M. D. (2015). “Modeling strongly non-gaussian non-stationary stochastic processes using the iterative translation approximation method and karhunen–loève expansion.” *Computers & Structures*, 161, 31–42.

Li, C.-Q., Firouzi, A., and Yang, W. (2016a). “Closed-form solution to first passage probability for nonstationary lognormal processes.” *Journal of Engineering Mechanics*, 142(12), 04016103.

Li, C.-Q., Lawanwisut, W., and Zheng, J. (2005). “Time-dependent reliability method to assess the serviceability of corrosion-affected concrete structures.” *Journal of Structural Engineering*, 131(11), 1674–1680.

Li, Q., Wang, C., and Ellingwood, B. R. (2015). “Time-dependent reliability of aging structures in the presence of non-stationary loads and degradation.” *Structural Safety*, 52, 132–141.

Li, Q., Wang, C., and Zhang, H. (2016b). “A probabilistic framework for hurricane damage assessment considering non-stationarity and correlation in hurricane actions.” *Structural Safety*, 59, 108–117.

Liu, P. and Der Kiureghian, A. (1986). “Multivariate distribution models with prescribed marginals and covariances.” *Probabilistic Engineering Mechanics*, 1(2), 105–112.

Lutes, L. D. and Sarkani, S. (2004). *Random vibrations: analysis of structural and mechanical systems*. Butterworth-Heinemann.

Melchers, R. (1999). *Structural reliability analysis and prediction*. Wiley, New York.

Mori, Y. and Ellingwood, B. R. (1993). “Reliability-based service-life assessment of aging concrete structures.” *Journal of Structural Engineering*, 119(5), 1600–1621.

- 491 Newland, D. E. (1993). *An introduction to random vibrations, spectral & wavelet analysis*
492 *(third edition)*. Pearson Education Limited, Edinburgh Gate, Harlow, England.
- 493 Pang, L. and Li, Q. (2016). “Service life prediction of rc structures in marine environment us-
494 ing long term chloride ingress data: Comparison between exposure trials and real structure
495 surveys.” *Construction and Building Materials*, 113, 979–987.
- 496 Pillai, T. M. and Veena, G. (2006). “Fatigue reliability analysis of fixed offshore structures: A
497 first passage problem approach.” *Journal of Zhejiang University, Science A*, 7(11), 1839–
498 1845.
- 499 Rackwitz, R. (2001). “Reliability analysis – a review and some perspectives.” *Structural*
500 *Safety*, 23(4), 365–395.
- 501 Ross, S. M. (2014). *Introduction to probability models (tenth edition)*. Academic press.
- 502 Tang, W. H. and Ang, A. (2007). *Probability concepts in engineering: Emphasis on applica-*
503 *tions to civil & environmental engineering*. Wiley Hoboken, NJ.
- 504 Wang, C., Li, Q., and Ellingwood, B. R. (2016). “Time-dependent reliability of ageing struc-
505 tures: an approximate approach.” *Structure and Infrastructure Engineering*, 12(12), 1566–
506 1572.
- 507 Wang, C. and Zhang, H. (2018). “Roles of load temporal correlation and deterioration-load
508 dependency in structural time-dependent reliability.” *Computers & Structures*, 194, 48–59.
- 509 Wang, C., Zhang, H., and Li, Q. (2017). “Reliability assessment of aging structures subjected
510 to gradual and shock deteriorations.” *Reliability Engineering & System Safety*, 161, 78–86.
- 511 Zheng, R. and Ellingwood, B. R. (1998). “Stochastic fatigue crack growth in steel structures
512 subject to random loading.” *Structural Safety*, 20(4), 303–323.

513 **List of Tables**

514 1 Probabilistic models of resistance and loads 27

TABLE 1: Probabilistic models of resistance and loads

Item	Mean	COV	Distribution
Initial resistance	$1.10\mathcal{R}_n$	0	Deterministic
Dead load	$1.00\mathcal{D}_n$	0	Deterministic
Lateral load	$0.50\mathcal{H}_n$	0.5	Lognormal

515 **List of Figures**

516 1 A comparison between a continuous load process and a discrete one. 29

517 2 Illustration of the outcrossing rate of stochastic process $X(t)$ relative to $\Omega(t)$. 30

518 3 Autocorrelation in hurricane load effects (after Ellingwood and Lee 2016). . . 31

519 4 Dependence of $R(\tau)$ on τ for different values of b 32

520 5 Autocorrelation functions in both $\mathcal{H}^*(t)$ (solid line) and Gaussian $\mathcal{H}(t)$ (dashed

521 line). 33

522 6 Sample sequences of $\mathcal{H}(t)$ (normalized by \mathcal{H}_n) and $\mathcal{H}^*(t)$, respectively. 34

523 7 Time-dependent failure probability for periods up to 50 years. 35

524 8 Upper tail behaviour of the CDF of \mathcal{H} (normalized by \mathcal{H}_n). 36

525 9 Dependence of failure probability on the autocorrelation in load process. . . 37

526 10 The CDF of $\max\{\mathcal{H}(t)\}$ (normalized by \mathcal{H}_n) during a unit time $\Delta = 1$ 38

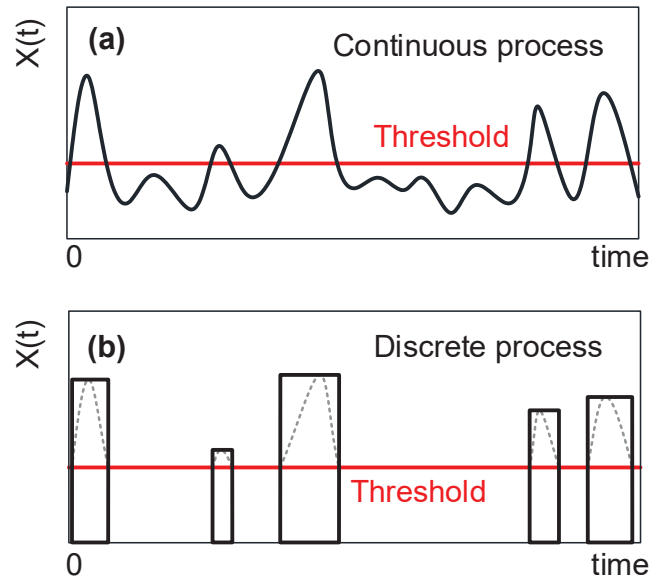


FIG. 1: A comparison between a continuous load process and a discrete one.

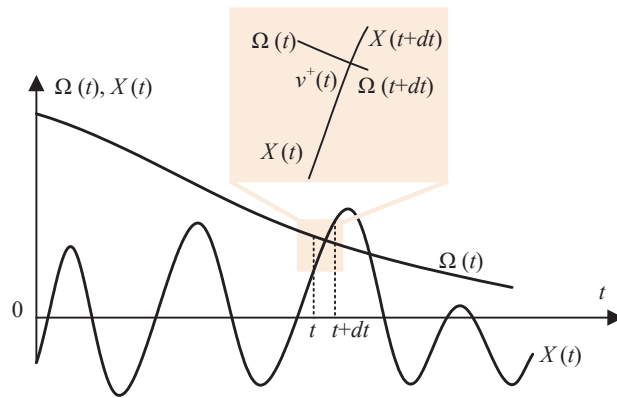


FIG. 2: Illustration of the outcrossing rate of stochastic process $X(t)$ relative to $\Omega(t)$.

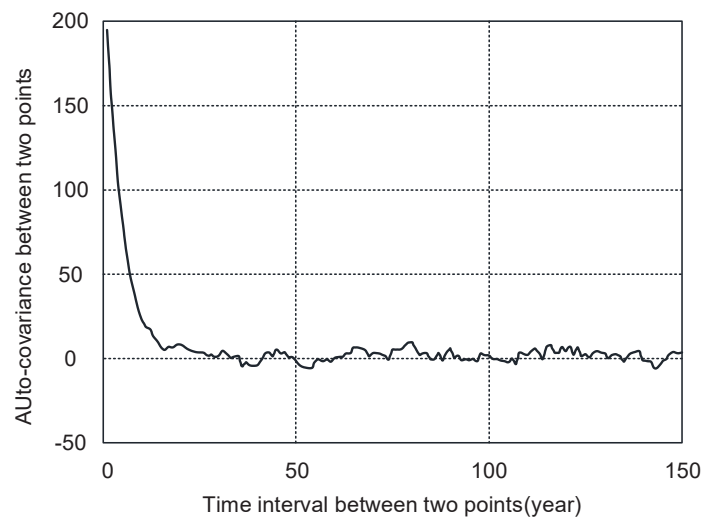


FIG. 3: Autocorrelation in hurricane load effects (after [Ellingwood and Lee 2016](#)).

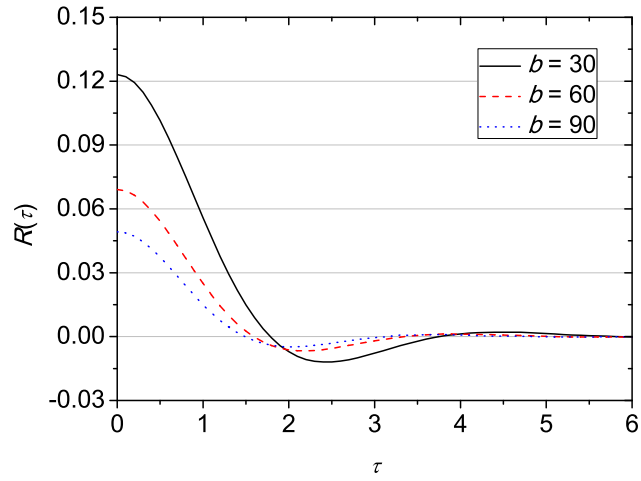


FIG. 4: Dependence of $R(\tau)$ on τ for different values of b .

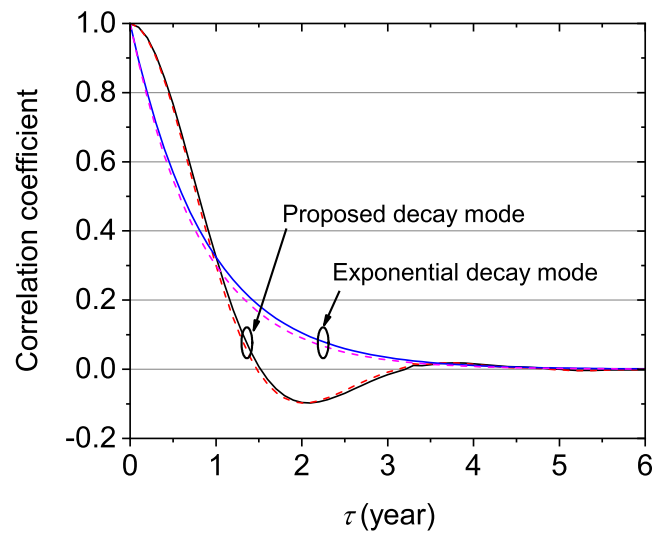


FIG. 5: Autocorrelation functions in both $\mathcal{H}^*(t)$ (solid line) and Gaussian $\mathcal{H}(t)$ (dashed line).

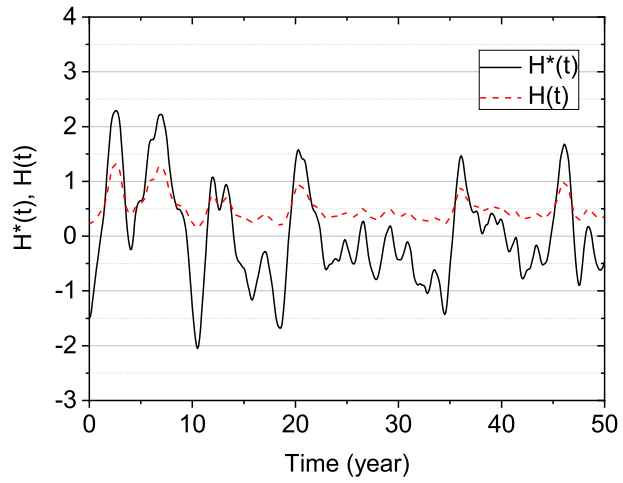
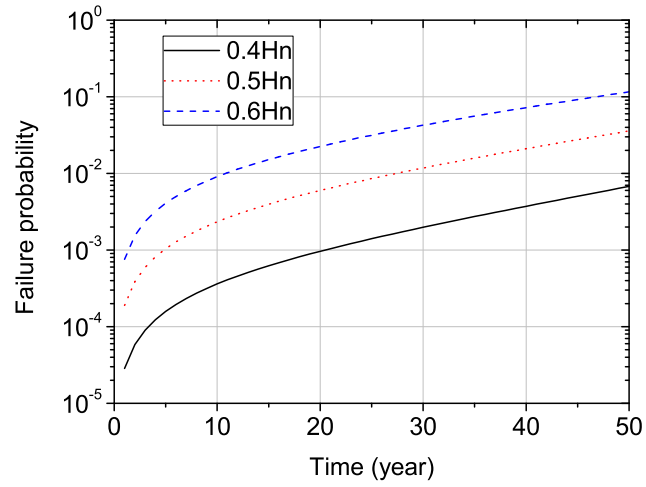
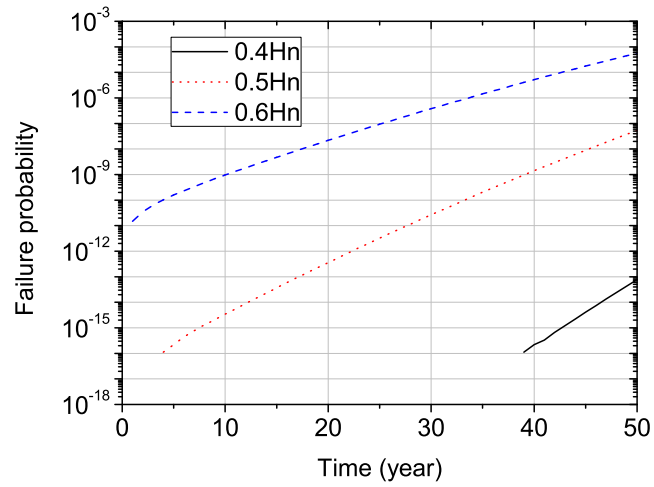


FIG. 6: Sample sequences of $\mathcal{H}(t)$ (normalized by \mathcal{H}_n) and $\mathcal{H}^*(t)$, respectively.



(a) \mathcal{H} follows a lognormal distribution as summarized in Table 1



(b) Assuming a Gaussian process of $\mathcal{H}(t)$

FIG. 7: Time-dependent failure probability for periods up to 50 years.

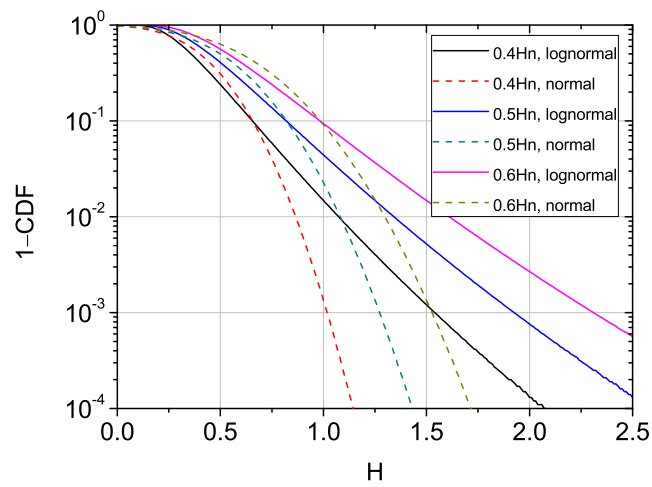


FIG. 8: Upper tail behaviour of the CDF of \mathcal{H} (normalized by \mathcal{H}_n).

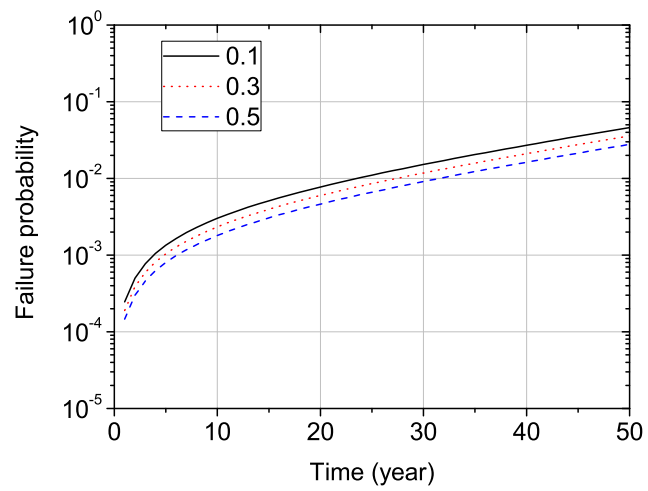


FIG. 9: Dependence of failure probability on the autocorrelation in load process.

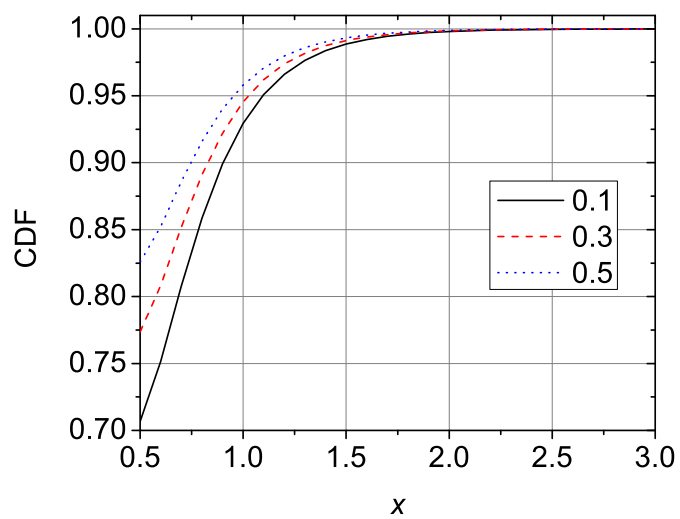


FIG. 10: The CDF of $\max\{\mathcal{H}(t)\}$ (normalized by \mathcal{H}_n) during a unit time $\Delta = 1$.